



Published in final edited form as:

Mult Scler. 2018 May ; 24(6): 739–749. doi:10.1177/1352458517707346.

Pittsburgh compound-B PET white matter imaging and cognitive function in late multiple sclerosis

Burcu Zeydan, M.D.^{1,2}, Val J. Lowe, M.D.², Christopher G. Schwarz, PhD.², Scott A. Przybelski³, Nirubol Tosakulwong³, Samantha M. Zuk², Matthew L. Senjem, M.S.^{2,4}, Jeffrey L. Gunter, PhD.⁴, Rosebud O. Roberts, M.B., Ch.B.^{1,3}, Michelle M. Mielke, Ph.D.^{1,3}, Eduardo E. Benarroch, M.D.¹, Moses Rodriguez, M.D.¹, Mary M. Machulda, PhD.⁵, Timothy G. Lesnick³, David S. Knopman, M.D.¹, Ronald C. Petersen, M.D., PhD.¹, Clifford R. Jack Jr, M.D.², Kejal Kantarci, M.D., M.S.², and Orhun H. Kantarci, M.D.¹

¹Mayo Clinic College of Medicine, Department of Neurology, Rochester, Minnesota, United States of America

²Mayo Clinic College of Medicine, Department of Radiology, Rochester, Minnesota, United States of America

³Mayo Clinic College of Medicine, Department of Health Sciences Research, Rochester, Minnesota, United States of America

⁴Mayo Clinic College of Medicine, Department of Information Technology, Rochester, Minnesota, United States of America

⁵Mayo Clinic College of Medicine, Department of Psychiatry and Psychology, Rochester, Minnesota, United States of America

Abstract

Background—There is growing interest in white matter (WM) imaging with PET.

Objectives—We studied the association of cognitive function in late MS with cortical and WM Pittsburgh compound B-PET (PiB-PET) binding.

Methods—In the population-based Mayo Clinic Study of Aging, 24 of 4869 participants had MS (12 underwent PiB-PET). Controls were age- and sex-matched (5:1). We used automated or semi-automated processing for quantitative image analyses and conditional logistic regression for group differences.

Correspondence to: Orhun H. Kantarci, M.D., Department of Neurology, Mayo Clinic and Foundation, 200 First Street, SW, Rochester, MN 55905, **Phone:** 507-284-4234, **Fax:** 507-266-4419, kantarci.orchun@mayo.edu.

Author contributions:

Drs. O.H. Kantarci, K. Kantarci and B. Zeydan had access to all of the clinical information from patients. *Study concept and design:* Drs. B. Zeydan, O.H. Kantarci and K. Kantarci. *Acquisition of data:* Drs V. Lowe, C. Schwarz, R. Roberts, M. Mielke, M. Machulda, D. Knopman, R. Petersen, C. Jack and K. Kantarci, Mr. S. Przybelski, M. Senjem and J. Gunter, T. Lesnick, Ms. N. Tosakulwong and S. Zuk. *Analysis and interpretation of data:* Drs. B. Zeydan, O.H. Kantarci, E. Benarroch and K. Kantarci. *Drafting of the manuscript:* Drs. B. Zeydan, O.H. Kantarci and K. Kantarci. *Critical Revision of the manuscript for important intellectual content:* Drs. O.H. Kantarci, K. Kantarci, E. Benarroch, C. Jack, M. Rodriguez, M. Machulda, D. Knopman, R. Petersen, V. Lowe, R. Roberts and M. Mielke. *Statistical analysis:* S. Przybelski, T. Lesnick and N. Tosakulwong. *Study Supervision:* Drs. O.H. Kantarci and K. Kantarci.

Results—MS patients had lower memory ($p=0.03$) and language ($p=0.02$) performance; smaller thalamic volumes ($p=0.003$), thinner temporal ($p=0.001$) and frontal ($p=0.045$) cortices on MRI than controls. There was no difference in global cortical PiB standardized uptake value ratios between MS and controls ($p=0.35$). PiB uptake was lower in areas of WM hyperintensities compared to normal appearing WM (NAWM) in MS ($p=0.0002$). Reduced PiB uptake in both the areas of WM hyperintensities ($r=0.65$; $p=0.02$), and NAWM ($r=0.69$; $p=0.01$) was associated with decreased visuospatial performance in MS.

Conclusions—PiB uptake in the cortex in late MS is not different from normal age matched controls. PiB uptake in the WM in late MS may be a marker of the large network structures' integrity such as those involved in visuospatial performance.

Keywords

Pittsburgh compound-B; PET; multiple sclerosis; myelin; cognition; thalamus

INTRODUCTION

Cognitive impairment affects more than half of the patients with multiple sclerosis (MS) including “benign MS”¹ and can be observed even in the early clinically isolated syndrome phase of the disease². Gray matter (GM) atrophy and high white matter (WM) and GM lesion loads are the core correlates of cognitive dysfunction in MS^{3,4}.

Neurodegeneration starts early in MS. As such, atrophy of the thalamus, the largest deep GM relay of the brain, can be observed in all ages including the earliest asymptomatic phase of MS (i.e. radiologically isolated syndrome-RIS) and worsens with time even in the absence of overt cognitive impairment⁵. Little is known about the imaging correlates of cognitive performance variation outside of overt impairment in MS. Studying late MS may allow one to compare cognitive health in MS to other age dependent causes of WM pathology.

Mild cognitive impairment (MCI) in older adults is commonly associated with cortical atrophy and deposition of β -amyloid, which is a pathological hallmark for Alzheimer Disease (AD)⁶. Therefore, cognitive difficulties in late MS could potentially be associated with β -amyloid deposition as well. [11C] Pittsburgh compound B (PiB) is a tracer that binds to fibrillary β -amyloid with high affinity, and is used in quantifying cortical β -amyloid plaques⁷. Advanced MRI techniques (e.g. diffusion tensor imaging) targeting the myelin component of brain parenchyma⁸ are not entirely myelin-specific. Intracellular and extracellular water, axons, and inflammatory infiltrates can contribute to this lack of specificity⁹. In contrast, several β -amyloid tracers including PiB can target myelin and bind to WM as an off target phenomenon independent of cortical β -amyloid deposition^{7,10–13}.

Here, we studied the cortical β -amyloid load, WM PiB binding, cortical thickness, thalamic volume and cognitive performance in patients with late MS compared to controls.

MATERIALS AND METHODS

Study population and consent (Figure-1)

We studied individuals enrolled in the Mayo Clinic Study of Aging (MCSA), a prospective population-based study of cognitive aging¹⁴ (See supplement). Of the 4869 MCSA participants between 2004 and 2015, 24 (0.5%) patients were previously diagnosed with MS. Diagnosis was confirmed with the most recent diagnostic criteria¹⁵ using expert clinical review by a neurologist (BZ) and an MS specialist (OHK). Each MS patient was age and sex matched to 5 controls without a demyelinating disease, MCI or dementia diagnosis from the same cohort.

The study protocol was approved by the Mayo Clinic and Olmsted Medical Center Institutional Review Boards. Every participant signed informed consent.

Neuropsychological testing

The neuropsychological battery assessed 4 cognitive domains of memory, language, attention-executive function, and visuospatial skills to calculate z-scores for individual tests', cognitive domains and a global cognitive z score as previously described¹⁴ (See supplement).

MRI acquisition and analyses

A standardized MRI imaging protocol was performed on 3.0 T MRI scanners (GE Healthcare). A T1-weighted 3D magnetization prepared rapid acquisition gradient-echo sequence and an axial T2-weighted fluid attenuated inversion recovery (FLAIR) sequence with an in plane resolution of 0.86×0.86 mm. and a slice thickness of 3.6 mm. (2.66 mm^3 resolution) were included in the protocol.

Previously described and validated structural MRI techniques of cortical thickness estimates from FreeSurfer (version 5.3)¹⁶ and thalamic volume estimates using an SPM12-based analysis¹⁷ were used. White matter hyperintensities (WMH) were quantified using a semi-automated segmentation algorithm on FLAIR as previously described¹⁸ (See supplement).

PiB-PET acquisitions and analyses

PET imaging was performed on a PET/CT scanner (DRX; GE Healthcare) operating in 3-dimensional mode. After the injection of [¹¹C] PiB (292–729 MBq) and after a 40-minute uptake period, a 20 minute PiB scan was acquired at 40 to 60 minutes post injection acquisition of four 5-minute dynamic frames. Dynamic PET images were generated (256 matrix, 300 mm field of view, $1.17 \text{ mm} \times 1.17 \text{ mm} \times 3.27 \text{ mm}$ voxel size, 4.48 mm^3 resolution) using an iterative reconstruction algorithm. Standard corrections for attenuation, scatter, randoms and decay were applied as well as a 5 mm Gaussian post filter. The images from the four dynamic frames were averaged to create a single static image. Previous data has shown that a 40–60 minute PiB acquisition has statistically equivalent accuracy in detecting PiB retention as compared to dynamic arterial sampling, carotid input sampling and delay-plateau phase acquisition periods ranging in total duration from 20–50 minutes¹⁹

An automated image processing pipeline, which includes registration of the PET image volume to each subject's own T1-weighted MRI for the segmentation of GM and WM was used as previously described²⁰. The global cortical PiB retention standard uptake value ratio (SUVr), with cerebellar GM uptake as the reference, was obtained from the bilateral parietal (including posterior cingulate and precuneus), temporal, prefrontal, orbitofrontal, and anterior cingulate GM regions. Participants were classified as PiB-positive or negative using a global cortical-to-cerebellar ratio cut off point of 1.42²¹.

Segmented WMH and the WM masks from FLAIR images in the subject's T1-weighted MRI space mentioned above, were used to derive the regional WM PiB SUVr for the WMH and the normal appearing WM (NAWM), from the PiB-PET images registered to subject's own T1-weighted MRI.

Statistical analyses

We described the demographic, clinical, and imaging characteristics of subjects in the control and MS groups using means and standard deviations for continuous variables, and counts and percentages for categorical variables. P-values comparing the control and MS groups were obtained using conditional logistic regression models to account for the matched case/control design. Associations of the imaging characteristics with cognitive function were additionally adjusted for WMH volume, and thalamic volume was further adjusted for total intracranial volume (See supplement).

RESULTS

Demographic and clinical characteristics (Table-1)

Of the 24 patients, 14 had relapsing remitting and 9 had progressive MS. One was unclassifiable. A subset of 16 patients had brain MRI, and 12 of the 16 with brain MRI also had PiB-PET. Except for an unexplained paucity of hypertension in MS, the groups did not differ in sex distribution, age at cognitive testing, age at imaging, *APOE* ϵ 4 carrier status, education level or atherosclerosis associated risk factors of WMH accumulation ($p > 0.05$).

Cognitive testing (Table-1)

Short Test of Mental Status scores²² or clinical dementia ratings did not differ between groups ($p > 0.05$). MS group had lower z-scores in the memory ($p = 0.03$) and language ($p = 0.02$) domains than controls. In the MS group, one patient fulfilled criteria for MCI and another patient fulfilled criteria for dementia⁶. None of the control individuals had MCI or dementia. The individual cognitive domain z-scores of these two patients are shown in table-1.

MRI characteristics (Table-2)

Expectedly, total WMH volume (corrected for total intracranial volume) was higher in patients with MS compared to the controls ($p = 0.001$). Median individual lesion volumes were not different between MS patients (23.9 mm³; interquartile range = 10.6–82.5 mm³) and controls (21.3 mm³; interquartile range = 10.6–58.5 mm³) (Wilcoxon rank-sum test;

$p=0.23$) suggesting any influence of partial volume averaging on WMH PiB SUVr measurements in these two groups was similar.

Greater WMH volume correlated with lower scores in all domains of cognitive performance but mainly with lower global z-scores (MS - correlation coefficient: -0.57 ; $p=0.03$, Controls - correlation coefficient: -0.29 ; $p=0.01$) and lower attention z-scores (MS - correlation coefficient: -0.56 ; $p=0.04$, Controls - correlation coefficient: -0.43 ; $p<0.01$). Although the correlations appeared to be stronger in MS patients compared to controls, the differences were not statistically significant ($p>0.05$).

Thalamic volume (corrected for total intracranial volume) was lower in the MS group compared to controls (unadjusted for WMH volume: $p=0.003$; adjusted for WMH volume: $p=0.03$) (Figure-2). Thalamic volume loss correlated mainly with lower attention-executive function z-scores in the MS group (correlation coefficient: 0.58 ; $p=0.02$). This correlation was attenuated after adjusting for WMH volume in the MS group (correlation coefficient: 0.42 ; $p=0.16$).

Temporal lobe cortical thickness (the largest cortical thickness of all lobes, Figure 3) was lower in the MS group compared to controls (unadjusted for WMH volume: $p=0.001$; adjusted for WMH volume: $p=0.006$). Frontal lobe cortical thickness was lower in the MS group compared to controls (unadjusted for WMH volume: $p=0.045$; adjusted for WMH volume: $p=0.03$). Parietal lobe cortical thickness was lower in the MS group compared to controls only after adjusting for WMH volume (unadjusted for WMH volume: $p>0.05$; adjusted for WMH volume: $p=0.04$). There was no difference in occipital cortical thickness between patients and controls adjusted or unadjusted for WMH volume ($p>0.05$). There was a suggestive but not significant correlation between temporal lobe cortical thinning and lower global cognitive z-scores (correlation coefficient: 0.46 ; $p=0.09$, correlation coefficient adjusted for WMH load: 0.52 ; $p=0.06$).

Cortical PiB SUVr (β -amyloid deposition) characteristics (Table 2)

There was no difference in global cortical PiB SUVr between patients with MS and controls in unadjusted ($p=0.35$) or WMH volume adjusted models ($p=0.49$). However, using the cortical-to-cerebellar ratio cut off point of 1.42, 10 controls (17%) had a positive global cortical PiB-PET scan while all MS patients were negative.

WM PiB SUVr characteristics (Figure-4)

In patients with MS, the WMH PiB SUVr (mean \pm SD: 1.58 ± 0.18) was lower compared to NAWM PiB SUVr (mean \pm SD: 1.66 ± 0.17) (predicted difference \pm SD: -0.083 ± 0.022 ; $p=0.0002$). Similarly, in controls, the WMH PiB SUVr (mean \pm SD: 1.65 ± 0.14) was lower compared to NAWM PiB SUVr (mean \pm SD: 1.72 ± 0.14) (predicted difference \pm SD: -0.067 ± 0.008 ; $p<0.0001$). Neither WMH PiB SUVrs (predicted difference \pm SD: -0.066 ± 0.042 ; $p=0.121$) nor NAWM PiB SUVrs (predicted difference \pm SD: -0.050 ± 0.042 ; $p=0.237$) differed between MS and control groups. When corrected for the differential presence of hypertension as a WMH risk factor, the results did not change. Given the small sample size additional multifactorial analyses were not feasible.

WMH PiB SUVR correlated with visuospatial performance z-scores in patients with MS (correlation coefficient: 0.65; $p=0.02$). NAWM PiB SUVR also correlated with visuospatial performance z-scores in patients with MS (correlation coefficient: 0.69; $p=0.01$). We did not observe similar correlations among controls, either in the WMH or NAWM PiB SUVRs (>0.05).

In figure 5, as follow up to quantitative analyses presented in figure 4, we show MRI and PiB-PET images from 1 patient with MS and 3 controls as visual examples of different densities of WMH risk factors, chosen to have similar PiB SUVRs to avoid a global inter-individual SUVR difference.

DISCUSSION

The frequency of MS (0.5%) in our study is concordant with the prevalence of MS in the same population (0.2%)²³. With a mean age at cognitive and imaging studies in the mid-60s and mean disease duration of 24 years, our study population was representative of a late MS population with also an older than expected age at onset of MS²³. Patients with earlier MS onset could have been too disabled or already deceased to join the MCSA. The study design enforced a limitation of not allowing us to generalize findings to younger MS, while focusing on “older” MS decreased the likelihood of active MS from confounding our results.

Within the typical age group of MS (younger than 55), the main cognitive difficulties are in processing speed, visual learning and complex sustained attention while verbal fluency problems affect 25% of MS patients²⁴. In our study patients with late MS performed worse in memory and language domains while increased WMH load, the hallmark of MS pathology on MRI, was associated with a lower global cognitive performance and decreased attention-executive function.

Late MS is characterized by normal PiB uptake in the cortex

PiB SUVR was calculated by using cerebellar GM as the reference region because cerebellum is relatively unaffected by the β -amyloid deposition⁷ or at least not as prone to β -pleated sheet configuration of amyloid²⁵. However even the cerebellum is not immune to amyloid pathology completely as can be seen in familial AD as opposed to sporadic AD or controls²⁶. Although the validity of cerebellar GM as a reference region for WM PiB uptake analyses was not previously established, we compared the PiB uptake in the cerebellar GM in MS vs matched controls and found no difference, unadjusted ($p=0.37$) or adjusted for WMH volume ($p=0.86$). Therefore we conclude that cerebellar GM PiB uptake is an acceptable reference for patients with MS within our study construct.

In the control group, there was evidence of cortical β -amyloid deposition without associated cognitive impairment in 17% of the participants. In contrast, none of the MS patients had a positive cortical PiB-PET scan despite the fact that MS group had worse cognitive performance than the control group. While MS patients can get Alzheimer’s disease (AD), it seems as if MS itself does not cause β -amyloid pathology in the cortex or having had MS might have been protective from cortical amyloid pathology. However, due to small sample size, one has to be cautious not to over-interpret our results. Alternatively, if PiB strongly

binds myelin, thinning of the limited amount of GM myelin could lead to significant enough loss of PiB binding. This could in return overwhelm a possibility to detect β -amyloid accumulation in GM that is otherwise present in older MS patients. Such a possibility of undetectable amyloid presence in the cortex can further be investigated longitudinally by an autopsy series.

Cortical thinning is present even at the first symptomatic manifestation of MS²⁷. In our study, most affected regions were the temporal and frontal lobes, the thicker cortical regions compared to the parietal and occipital lobes. The frontal and temporal lobes contain multimodal association areas that, like the thalamus, are interconnected with multiple cortical areas via a large number of WM tracts prone to damage in MS. Our study supports the previous associations between structural and functional changes in the temporal lobe and cognitive performance in MS²⁸. Since the association between temporal lobe cortical thinning in late MS and a lower global cognitive z score in our study became stronger when corrected for WMH load, it is likely that cortical lesions independently contribute to temporal and frontal atrophy in MS.

There is about 2-fold increase in the number of lesions detected and with significant more inter-rater agreement in 7T vs 3T MRI²⁹. As such, 7T MRI studies identify cortical lesions in 97% of patients with MS³⁰ and potentially are more suitable for such precise analyses than 3T MRI studies like ours. Therefore we specifically did not analyze the impact of cortical lesions in relation to PiB-PET findings. However, our findings suggest that not just the global cortical lesion load but also the distribution of local cortical atrophy should be analyzed in relation to specific cognitive domains in MS.

Previous findings suggest that deep GM and especially thalamic atrophy is a structural marker associated with cognitive processing difficulties in MS^{31, 32}. Loss of thalamic volume may reflect a reduction of neuronal density due to cell intrinsic mechanisms, loss of anterograde and retrograde connectivity due to WM lesions, or combination thereof^{33, 34}. We show that thalamic volume correlates with performance in attention-executive function in MS, highlighting role of thalamus in attention³⁵. The weakening of this correlation after correcting for WMH load suggests that the involvement of thalamo cortical projections, rather than a direct thalamic involvement alone, is the likely driver of this association. PiB-PET can potentially be utilized to study the association between these projections and cognitive function in MS.

Reduced PiB uptake in the WM as a potential global marker of WM integrity is associated with decreased visuospatial performance

PET is a promising alternative for myelin imaging^{9, 10, 12, 13, 36, 37}. Human PET studies highlighted the potential sensitivity of PiB in detecting white matter integrity¹¹ and its reliability for use in longitudinal evaluations³⁸. PiB uptake in WM was partly explained by binding of PiB to the beta-sheet structure of myelin basic protein,¹¹ which is degraded in WMH of various causes including MS³⁹. A micro PET study showed a high sensitivity for PiB in detecting remyelination in lyssolecithin induced rat demyelination model¹³. In MS, a reduction in PiB uptake is more prominent in periventricular WM lesions⁴⁰.

Consistent with previous studies^{9, 41}, we demonstrated that PiB differentiated WMH from NAWM. The reduction of PiB uptake in WMH compared to NAWM may be a result of disruption of the beta-sheet structure or a measure of total amount of myelin loss. As presented in individual examples, WM lesions in the patient with MS and additional WMH risk factors were associated with practically absent PiB uptake when compared to individuals with non-MS WMH risk factors alone. As expected from this observation, there was an intriguingly lower PiB uptake within WMH in MS than in controls within the sample size limits.

While the static PiB-PET quantification approach provides higher white matter/grey matter contrast it also shows poor reproducibility compared to a dynamic approach³⁸. A static SUVr method was preferred over dynamic sampling for 2 reasons. Dynamic scanning requires much longer camera time and hence is much more expensive and therefore not feasible in a population-based study of thousands of individuals like the MCSA. Longer scan times impose much greater subject burden making it not feasible for a volunteer-based longitudinal study such as ours.

Per the original MRI protocol, we did not obtain gadolinium-T1 imaging and did not study the association between PiB binding and active MS lesions. It likely would not have mattered since the frequency of gadolinium enhancing lesions decrease dramatically after 40 years of age⁴².

Visuospatial processing requires one of the largest network organizations of the central nervous system with relatively long tracts connecting parietal multimodal association areas to lateral prefrontal cortex and medial-inferior temporal cortices with occipital lobes. Therefore, this network would be very prone to disruption by WM damage. In MS, WM damage is not limited to lesions and can be seen in the NAWM. We found that PiB uptake in areas of WMH and NAWM correlated with visuospatial performance in MS. Visuospatial processing changes in MS probably reflects disrupted neuronal connectivity in association areas due to WM damage reflected in PiB-PET measurements. While our finding highlights the potential sensitivity of PiB-PET in detecting overall WM damage in MS, the final interpretation will require confirmation in a larger number of cases, younger patients and longitudinal studies.

Supplementary Material

Refer to Web version on PubMed Central for supplementary material.

Acknowledgments

Potential Conflict of interests:

Dr. B. Zeydan: Received support from the Turkish Neurological Society.

Dr. V. Lowe: Reports grants from NIH, grants from Liston Foundation, grants from The Elsie and Marvin Dekelboun Family Foundation, during the conduct of the study; personal fees from Bayer Pharmaceuticals, grants from GE Health Care, grants from Siemens Molecular Imaging, grants from AVID Radiopharmaceuticals, personal fees from Piramal Imaging, outside the submitted work.

Dr. C. Schwarz, Mr. S. Przybelski, Ms. N. Tosakulwong, Ms. S. Zuk, Mr. J. Gunter, Dr. R. Roberts, Dr. M. Mielke, Dr. E. Benarroch, Dr. M. Rodriguez, Dr. M. Machulda and Mr. T. Lesnick: Nothing to disclose.

Mr. M. Senjem: Equity/options ownership in medical companies: Gilead Sciences, Inc., Inovio Pharmaceuticals, Medtronic, and PAREXEL International Corporation.

Dr. D.S. Knopman: Serves on a Data Safety Monitoring Board for Lundbeck Pharmaceuticals and for the Dominantly Inherited Alzheimer's Disease Treatment Unit. He is participating in clinical trials sponsored by Lilly Pharmaceuticals and Tau Rx Pharmaceuticals. He receives research support from the NIH.

Dr. R. Petersen: Chaired a Data Monitoring Committee of Pfizer, Inc. and Janssen Alzheimer Immunotherapy and serves as a consultant for Hoffman La Roche, Inc., Merck, Inc., Genentech, Inc., Biogen, Inc., Eli Lilly and Co. and receives research support from the NIH (P50 AG016574 [PI] and U01 AG006786 [PI], R01 AG011378 [Co-I], and U01 AG024904 [Co-I]).

Dr. C. Jack: Reports consulting services for Eli Lilly Co, funding from the NIH (R01 AG011378, U01 AG024904, R01 AG041851, R01 AG037551, R01 AG043392, and U01 AG006786) and research support from the Alexander Family Professorship of Alzheimer's Disease Research.

Dr. K. Kantarci: Serves on the data safety monitoring board for Pfizer Inc. and Janssen Alzheimer's Immunotherapy Takeda Global Research & Development Center, Inc.; and she is funded by the NIH.

Dr. O. H. Kantarci: Gave and organized scientific presentations at meetings supported by Novartis Pharmaceuticals, but has received no personal compensation; presented as an invited professor in Biogen Pharmaceuticals, but received no personal compensation.

Funding/Support:

This study was funded by the NIH [R01 AG040042, P50 AG016574, U01 AG006786, C06 RR018898], The Minnesota Partnership for Biotechnology and Medical Genomics, The Elsie and Marvin Dekelboum Family Foundation, and the Robert H. and Clarice Smith and Abigail Van Buren Alzheimer's Disease Research Program. The funding sources had no role in study design, collection, analysis, interpretation, or decision to submit this paper. The corresponding author had full access to all the data in the study and had final responsibility for the decision to submit for publication.

References

1. Amato MP, Zipoli V, Goretti B, et al. Benign multiple sclerosis: cognitive, psychological and social aspects in a clinical cohort. *J Neurol*. 2006; 253:1054–9. [PubMed: 16609810]
2. Achiron A, Barak Y. Cognitive impairment in probable multiple sclerosis. *J Neurol Neurosurg Psychiatry*. 2003; 74:443–6. [PubMed: 12640060]
3. Rao SM, Leo GJ, Ellington L, Nauertz T, Bernardin L, Unverzagt F. Cognitive dysfunction in multiple sclerosis. II. Impact on employment and social functioning. *Neurology*. 1991; 41:692–6. [PubMed: 1823781]
4. Rocca MA, Amato MP, De Stefano N, et al. Clinical and imaging assessment of cognitive dysfunction in multiple sclerosis. *Lancet Neurol*. 2015; 14:302–17. [PubMed: 25662900]
5. Azevedo CJ, Overton E, Khadka S, et al. Early CNS neurodegeneration in radiologically isolated syndrome. *Neurol Neuroimmunol Neuroinflamm*. 2015; 2:e102. [PubMed: 25884012]
6. Petersen RC, Aisen P, Boeve BF, et al. Mild cognitive impairment due to Alzheimer disease in the community. *Ann Neurol*. 2013; 74:199–208. [PubMed: 23686697]
7. Klunk WE, Engler H, Nordberg A, et al. Imaging brain amyloid in Alzheimer's disease with Pittsburgh Compound-B. *Ann Neurol*. 2004; 55:306–19. [PubMed: 14991808]
8. Filippi M, Rocca MA, Barkhof F, et al. Association between pathological and MRI findings in multiple sclerosis. *Lancet Neurol*. 2012; 11:349–60. [PubMed: 22441196]
9. Bodini B, Veronese M, Garcia-Lorenzo D, et al. Dynamic imaging of individual remyelination profiles in multiple sclerosis. *Ann Neurol*. 2016
10. Stankoff B, Wang Y, Bottlaender M, et al. Imaging of CNS myelin by positron-emission tomography. *Proc Natl Acad Sci U S A*. 2006; 103:9304–9. [PubMed: 16754874]

11. Stankoff B, Freeman L, Aigrot MS, et al. Imaging central nervous system myelin by positron emission tomography in multiple sclerosis using [methyl-(1)(1)C]-2-(4'-methylaminophenyl)-6-hydroxybenzothiazole. *Ann Neurol.* 2011; 69:673–80. [PubMed: 21337603]
12. Wang Y, Wu C, Capriello AV, et al. In vivo quantification of myelin changes in the vertebrate nervous system. *J Neurosci.* 2009; 29:14663–9. [PubMed: 19923299]
13. Faria Dde P, Copray S, Sijbesma JW, et al. PET imaging of focal demyelination and remyelination in a rat model of multiple sclerosis: comparison of [11C]MeDAS, [11C]CIC and [11C]PIB. *Eur J Nucl Med Mol Imaging.* 2014; 41:995–1003. [PubMed: 24499866]
14. Roberts RO, Geda YE, Knopman DS, et al. The Mayo Clinic Study of Aging: design and sampling, participation, baseline measures and sample characteristics. *Neuroepidemiology.* 2008; 30:58–69. [PubMed: 18259084]
15. Polman CH, Reingold SC, Banwell B, et al. Diagnostic criteria for multiple sclerosis: 2010 revisions to the McDonald criteria. *Ann Neurol.* 2011; 69:292–302. [PubMed: 21387374]
16. Dale AM, Fischl B, Sereno MI. Cortical surface-based analysis. I. Segmentation and surface reconstruction. *Neuroimage.* 1999; 9:179–94. [PubMed: 9931268]
17. Schwarz CG, Gunter JL, Wiste HJ, et al. A large-scale comparison of cortical thickness and volume methods for measuring Alzheimer's disease severity. *Neuroimage Clin.* 2016; 11:802–12. [PubMed: 28050342]
18. Raz L, Jayachandran M, Tosakulwong N, et al. Thrombogenic microvesicles and white matter hyperintensities in postmenopausal women. *Neurology.* 2013; 80:911–8. [PubMed: 23408873]
19. Price JC, Klunk WE, Lopresti BJ, et al. Kinetic modeling of amyloid binding in humans using PET imaging and Pittsburgh Compound-B. *J Cereb Blood Flow Metab.* 2005; 25:1528–47. [PubMed: 15944649]
20. Jack CR Jr, Lowe VJ, Senjem ML, et al. 11C PiB and structural MRI provide complementary information in imaging of Alzheimer's disease and amnesic mild cognitive impairment. *Brain.* 2008; 131:665–80. [PubMed: 18263627]
21. Jack CR Jr, Wiste HJ, Weigand SD, et al. Defining imaging biomarker cut points for brain aging and Alzheimer's disease. *Alzheimers Dement.* 2016
22. Tang-Wai DF, Knopman DS, Geda YE, et al. Comparison of the short test of mental status and the mini-mental state examination in mild cognitive impairment. *Arch Neurol.* 2003; 60:1777–81. [PubMed: 14676056]
23. Mayr WT, Pittock SJ, McClelland RL, Jorgensen NW, Noseworthy JH, Rodriguez M. Incidence and prevalence of multiple sclerosis in Olmsted County, Minnesota, 1985–2000. *Neurology.* 2003; 61:1373–7. [PubMed: 14638958]
24. Rao SM, Leo GJ, Bernardin L, Unverzagt F. Cognitive dysfunction in multiple sclerosis. I. Frequency, patterns, and prediction. *Neurology.* 1991; 41:685–91. [PubMed: 2027484]
25. Styren SD, Kamboh MI, DeKosky ST. Expression of differential immune factors in temporal cortex and cerebellum: the role of alpha-1-antichymotrypsin, apolipoprotein E, and reactive glia in the progression of Alzheimer's disease. *J Comp Neurol.* 1998; 396:511–20. [PubMed: 9651008]
26. Knight WD, Okello AA, Ryan NS, et al. Carbon-11-Pittsburgh compound B positron emission tomography imaging of amyloid deposition in presenilin 1 mutation carriers. *Brain.* 2011; 134:293–300. [PubMed: 21084313]
27. Calabrese M, Atzori M, Bernardi V, et al. Cortical atrophy is relevant in multiple sclerosis at clinical onset. *J Neurol.* 2007; 254:1212–20. [PubMed: 17361339]
28. Benedict RH, Ramasamy D, Munschauer F, Weinstock-Guttman B, Zivadinov R. Memory impairment in multiple sclerosis: correlation with deep grey matter and mesial temporal atrophy. *J Neurol Neurosurg Psychiatry.* 2009; 80:201–6. [PubMed: 18829629]
29. Nielsen AS, Kinkel RP, Tinelli E, Benner T, Cohen-Adad J, Mainero C. Focal cortical lesion detection in multiple sclerosis: 3 Tesla DIR versus 7 Tesla FLASH-T2. *J Magn Reson Imaging.* 2012; 35:537–42. [PubMed: 22045554]
30. Harrison DM, Roy S, Oh J, et al. Association of Cortical Lesion Burden on 7-T Magnetic Resonance Imaging With Cognition and Disability in Multiple Sclerosis. *JAMA Neurol.* 2015; 72:1004–12. [PubMed: 26192316]

31. Houtchens MK, Benedict RH, Killiany R, et al. Thalamic atrophy and cognition in multiple sclerosis. *Neurology*. 2007; 69:1213–23. [PubMed: 17875909]
32. Schoonheim MM, Popescu V, Rueda Lopes FC, et al. Subcortical atrophy and cognition: sex effects in multiple sclerosis. *Neurology*. 2012; 79:1754–61. [PubMed: 23019265]
33. Cifelli A, Arridge M, Jezzard P, Esiri MM, Palace J, Matthews PM. Thalamic neurodegeneration in multiple sclerosis. *Ann Neurol*. 2002; 52:650–3. [PubMed: 12402265]
34. Henry RG, Shieh M, Amirbekian B, Chung S, Okuda DT, Pelletier D. Connecting white matter injury and thalamic atrophy in clinically isolated syndromes. *J Neurol Sci*. 2009; 282:61–6. [PubMed: 19394969]
35. de Bourbon-Teles J, Bentley P, Koshino S, et al. Thalamic control of human attention driven by memory and learning. *Curr Biol*. 2014; 24:993–9. [PubMed: 24746799]
36. Matias-Guiu JA, Cabrera-Martin MN, Matias-Guiu J, et al. Amyloid PET imaging in multiple sclerosis: an (18)F-florbetaben study. *BMC Neurol*. 2015; 15:243. [PubMed: 26607782]
37. Matias-Guiu JA, Cabrera-Martin MN, Oreja-Guevara C, Carreras JL, Matias-Guiu J. PiB and other amyloid-PET tracers for the study of white matter and multiple sclerosis. *Ann Neurol*. 2016
38. Veronese M, Bodini B, Garcia-Lorenzo D, et al. Quantification of [(11)C]PiB-PET for imaging myelin in the human brain: a test-retest reproducibility study in high-resolution research tomography. *J Cereb Blood Flow Metab*. 2015; 35:1771–82. [PubMed: 26058700]
39. Murray ME, Vemuri P, Preboske GM, et al. A quantitative postmortem MRI design sensitive to white matter hyperintensity differences and their relationship with underlying pathology. *J Neuropathol Exp Neurol*. 2012; 71:1113–22. [PubMed: 23147507]
40. Glodzik L, Rusinek H, Li J, et al. Reduced retention of Pittsburgh compound B in white matter lesions. *Eur J Nucl Med Mol Imaging*. 2015; 42:97–102. [PubMed: 25331458]
41. Goodheart AE, Tamburo E, Minhas D, et al. Reduced binding of Pittsburgh Compound-B in areas of white matter hyperintensities. *Neuroimage Clin*. 2015; 9:479–83. [PubMed: 26594630]
42. Tortorella C, Bellacosa A, Paolicelli D, et al. Age-related gadolinium-enhancement of MRI brain lesions in multiple sclerosis. *J Neurol Sci*. 2005; 239:95–9. [PubMed: 16209877]

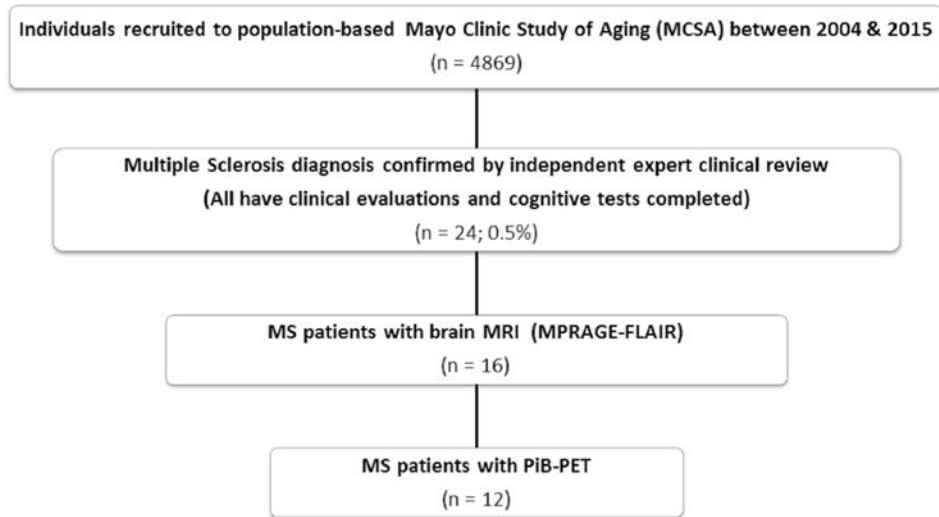


Figure-1. Study cohort. All 24 patients consented for cognitive studies; 16 of the 24 consented for MRI studies and 12 of the 16 patients with MRI also consented for PET studies.

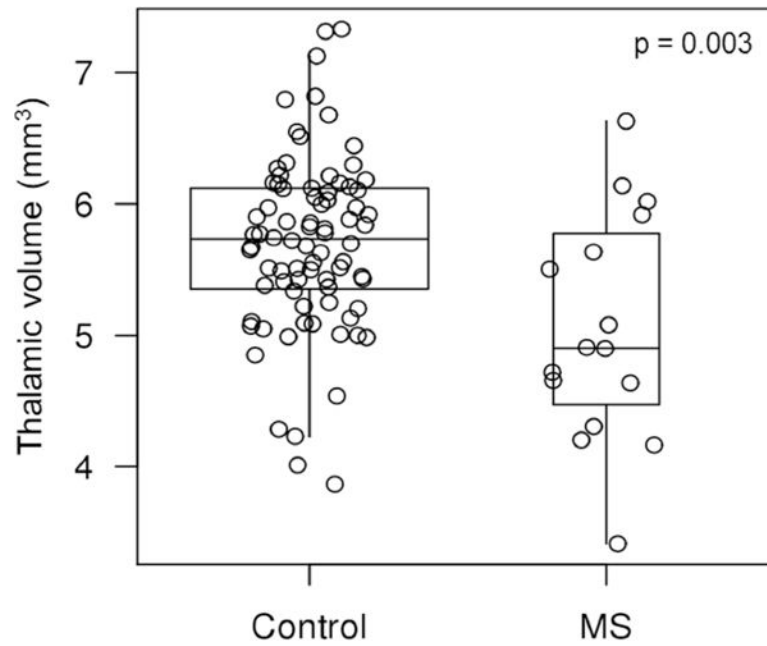


Figure-2.

Thalamic volumes of patients with MS and controls are shown in boxplots ranging from 25th to 75th percentile (the middle line shows the median). The vertical lines (whiskers) above and below the box extend a distance of $1.5 \times$ interquartile range or to the extreme value of the data in that direction, whichever comes first. Unadjusted (for white matter hyperintensity volume or total intracranial volume) p-value is shown. Patients with MS have lower thalamic volume compared to controls.

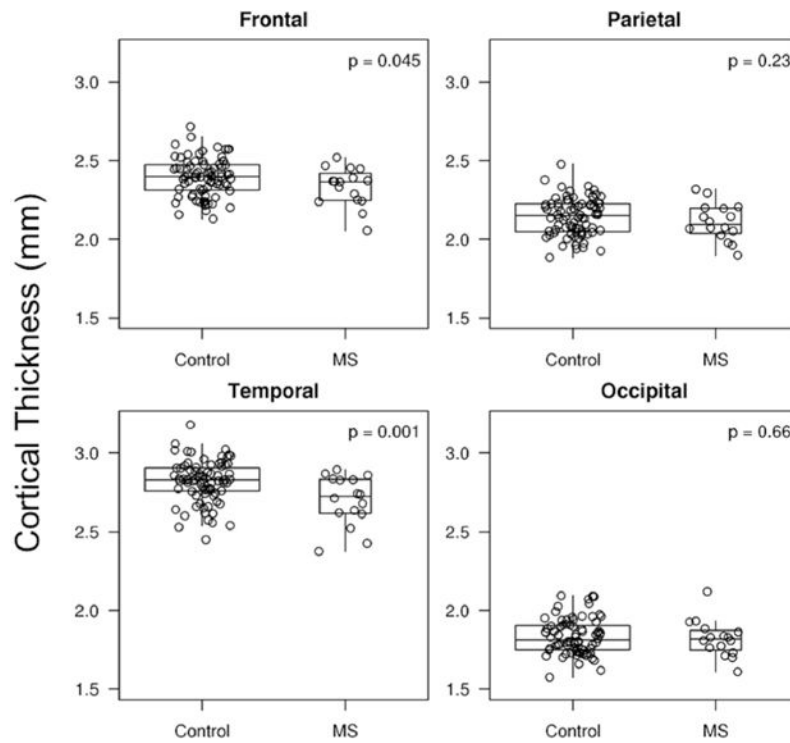


Figure-3.

Cortical thickness of patients with MS and controls (frontal, parietal, temporal and occipital lobes) are shown in boxplots ranging from 25th to 75th percentile (the middle line shows the median). The vertical lines (whiskers) above and below the box extend a distance of $1.5 \times$ interquartile range or to the extreme value of the data in that direction, whichever comes first. Unadjusted (for white matter hyperintensity volume) p-value is shown. Patients with MS have lower cortical thickness in temporal and frontal lobes, compared to controls.

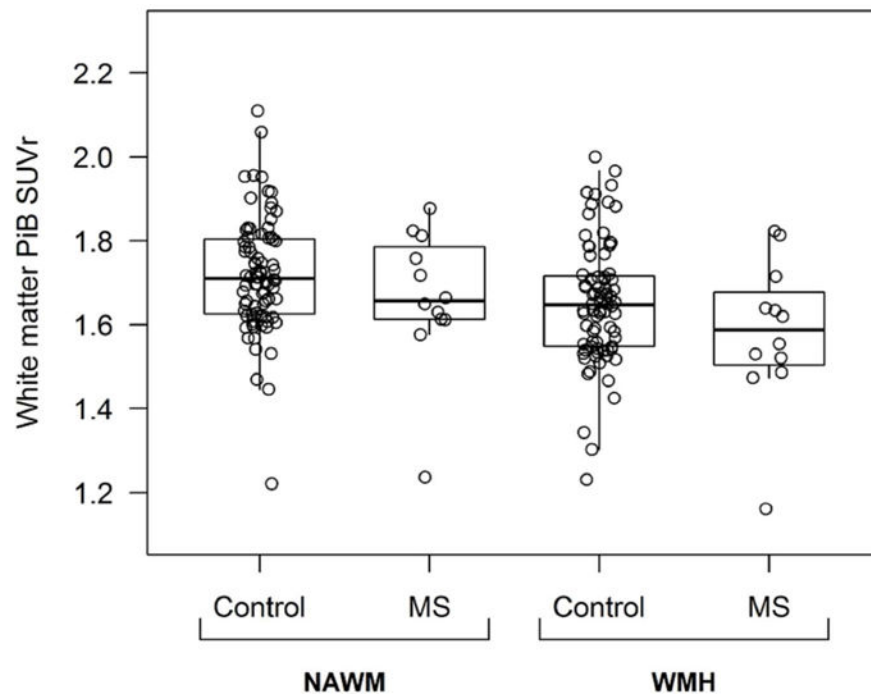


Figure-4.

PiB SUVR in NAWM and WMH are shown in boxplots ranging from 25th to 75th percentile (the middle line shows the median). The vertical lines (whiskers) above and below the box extend a distance of $1.5 \times$ interquartile range or to the extreme value of the data in that direction, whichever comes first in four groups: NAWM controls, NAWM MS patients, WMH controls, and WMH MS patients.

NAWM = Normal appearing white matter; WMH = White matter hyperintensity; PiB = [11C] Pittsburgh compound-B; SUVR = Standardized uptake value ratio

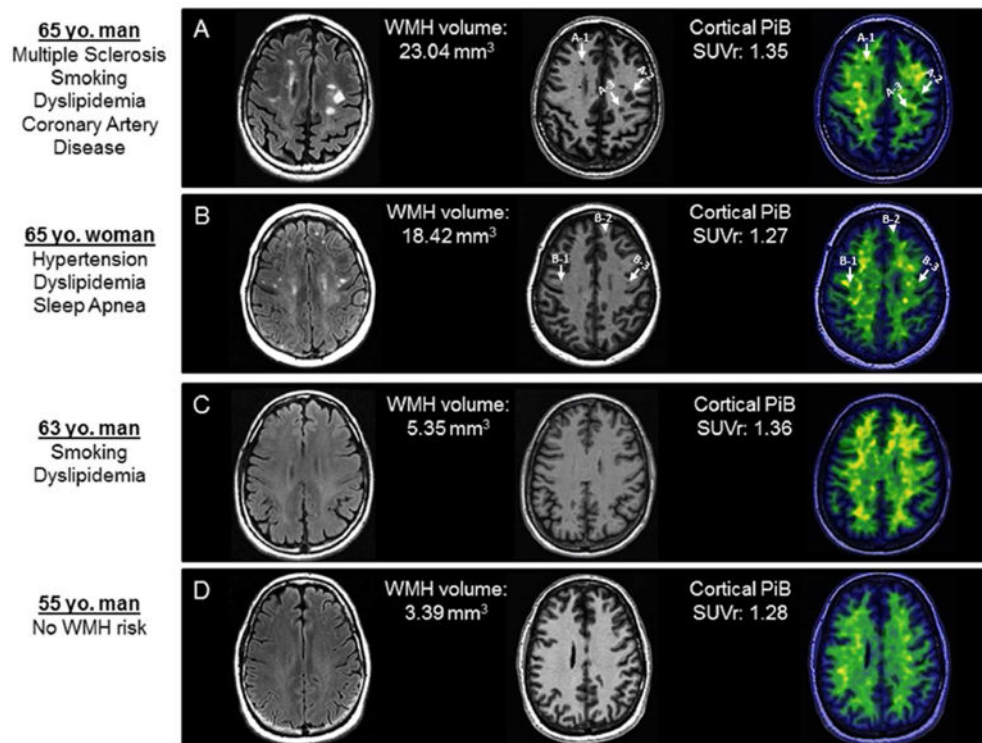


Figure-5.

Example individuals with gradually decreasing WMH load, but similar global cortical PiB SUVR are shown. PiB SUVR measurements on positron emission tomography (PET) for individual lesions are calculated from the center of the lesions as identified in the co-registered MPRAGE images and presented as examples for participants A and B. We selected these patients as examples after the quantitative analyses and a blinded visual analysis was not conducted. **A.** 65 year-old man with multiple sclerosis with additional WMH risk factors of smoking, dyslipidemia and coronary artery disease. Typical demyelinating lesions on T2 Flair image appear as T1 hypointensities (black holes) on a magnetization-prepared rapid acquisition gradient echo (MPRAGE) slice. Example PiB SUVR measurements for individual lesions are: A1=1.47, A2=1.40, A3=1.22. **B.** 65 year-old woman without MS and with WMH risk factors of hypertension, dyslipidemia and obstructive sleep apnea. Despite similar WMH load to the patient with MS on T2 Flair image, less prominent corresponding T1 hypointensities on the MPRAGE slice and less prominent reduced PiB uptake of the same lesions on the co-registered PET image is observed. Example PiB SUVR measurements for individual lesions are: B1=1.90, B2=1.63, B3=1.68. **C.** 63 year-old man without MS and with WMH risk factors of smoking and dyslipidemia. **D.** 55 year-old man without any WMH risk factors. In both examples C and D with significantly lower WMH loads compared to the patient with MS on T2 Flair image, there are no T1 hypointensities on MPRAGE images or focally reduced PiB uptake. WMH = White matter hyperintensity; PiB = [11C] Pittsburgh compound-B; SUVR = Standardized uptake value ratio

Table 1

Demographic and clinical characteristics of patients with MS and age sex matched ($\times 5$) clinically normal individuals from the population-based cohort.

	Control n = 120	MS n = 24 [‡]	<i>p</i> [†]
Women (%)	70 (58)	14 (58)	1.00
Age at cognitive testing (mean \pm SD)	66.13 (10.92)	66.00 (11.20)	0.57
Age at imaging (mean \pm SD)	64.50 (10.2)	64.30 (10.5)	0.63
Education (year) (mean \pm SD)	14.52 (2.33)	13.83 (4.10)	0.15
<i>APOE</i> $\epsilon 4$ carriers (%)	33 (29)	8 (38)	0.39
Non-MS WMH risk factors			
Smoking	46 (38)	12 (52)	0.15
Hypertension	65 (54)	6 (26)	0.01
Diabetes	13 (11)	1 (4)	0.38
Dyslipidemia	82 (68)	17 (74)	0.47
Congestive heart failure	5 (4)	0	0.99
Coronary artery disease	25 (21)	3 (13)	0.37
Atrial fibrillation/flutter	6 (5)	1 (4)	0.86
Obstructive Sleep Apnea	22 (18)	3 (13)	0.48
STMS (mean \pm SD)	35.48 (2.12)	34.61 (3.61)	0.10
CDR Sum of Boxes (mean \pm SD)	0.07 (0.36)	0.30 (0.75)	0.07
z-Global (mean \pm SD)	0.24 (0.96)	-0.05 (1.23)	0.11
z-Memory (mean \pm SD)	0.25 (0.92)	-0.17 (1.19)	0.03
z-Language (mean \pm SD)	0.07 (0.94)	-0.37 (1.30)	0.02
z-Attention-executive (mean \pm SD)	0.22 (0.98)	0.07 (1.40)	0.33
z-Visuospatial (mean \pm SD)	0.20 (0.95)	0.00 (1.10)	0.38

[†] Conditional logistic model accounting for the matching

[‡] One patient with MS has missing education and z-domain data. One patient with MS and MCI had z-Memory score of -1.69, z- Language score of -2.39, and z-Visuospatial score of -0.39 while z-Attention-executive score was not available. One patient with MS and dementia had z-Memory score of -3.04 while z-Language, z-Attention-executive and z-Visuospatial scores were not available. *APOE* = Apolipoprotein E; CDR = Clinical dementia rating; STMS = Short test of mental status score; WMH = White matter hyperintensity

Table 2

Imaging characteristics of patients with MS and age sex matched ($\times 5$) clinically normal individuals from the population-based cohort.

Imaging characteristics (Mean \pm SD)	Control n = 80*	MS n = 16*	p^{\ddagger}	$p^{\ddagger\ddagger}$
WMH volume (mm ³)	9.33 (14.93)	19.63 (25.27)	0.001 \ddagger	—
Thalamic volume (mm ³)	5.70 (0.67)	5.05 (0.86)	0.003	0.03 $\ddagger\ddagger$
Frontal cortical thickness (mm)	2.39 (0.12)	2.33 (0.12)	0.045	0.03
Parietal cortical thickness (mm)	2.14 (0.12)	2.11 (0.12)	0.23	0.04
Occipital cortical thickness (mm)	1.83 (0.11)	1.82 (0.12)	0.66	0.26
Temporal cortical thickness (mm)	2.82 (0.13)	2.70 (0.16)	0.001	0.006
Global cortical PiB SUVR (cerebellum scaled)*	1.33 (0.21)	1.29 (0.08)	0.35 \ddagger	0.49

* 16 patients with MS had MRI completed and were matched to 80 controls. 12 MS patients had PET studies and were matched to 60 controls. The single patient with MS and MCI did not have an MRI or PET so was not included in the analyses. The single patient with MS and dementia did not have a PET study but completed an MRI. In the patient with MS and dementia WMH volume was 14.27 mm³, thalamic volume was 4.31 mm³, frontal cortical thickness was 2.16 mm, parietal cortical thickness was 2.05 mm, occipital cortical thickness was 1.73 mm and temporal cortical thickness was 2.68 mm.

\ddagger Conditional logistic model accounting for the matching

$\ddagger\ddagger$ p value adjusted for WMH volume

\ddagger log transformation of the variable due to skewness

$\ddagger\ddagger$ p value adjusted for WMH volume and total intracranial volume (TIV)

PiB = [11C] Pittsburgh Compound B; SUVR = Standardized uptake value ratio; WMH = White matter hyperintensity